

# 1 **Motor improvement estimation and task adaptation for** 2 **personalized robot-aided therapy: a feasibility study**

3 Christian Giang<sup>a</sup>, Elvira Pirondini<sup>b,c,\*</sup>, Nawal Kinany<sup>a,b,c,\*</sup>, Camilla Pierella<sup>a,\*</sup>,  
4 Alessandro Panarese<sup>d</sup>, Martina Coscia<sup>e</sup>, Jenifer Miehlsbradt<sup>a</sup>, Cécile Magnin<sup>f</sup>,  
5 Pierre Nicolo<sup>f,g</sup>, Adrian Guggisberg<sup>f,g</sup> and Silvestro Micera<sup>a,d</sup>

6 <sup>a</sup>Bertarelli Foundation Chair in Translational Neuroengineering, Center for Neuroprosthetics and  
7 Institute of Bioengineering, School of Engineering, École Polytechnique Fédérale de Lausanne  
8 (EPFL), Lausanne, 1015, Switzerland.

9 <sup>b</sup>Institute of Bioengineering/Center for Neuroprosthetics, Ecole Polytechnique Fédérale de Lausanne  
10 (EPFL), Lausanne, Switzerland

11 <sup>c</sup>Department of Radiology and Medical Informatics, University of Geneva, Geneva, Switzerland

12 <sup>d</sup>Translational Neural Engineering Area, The Biorobotics Institute, Scuola Superiore Sant'Anna, Pisa,  
13 56025, Italy.

14 <sup>e</sup>Wyss Center for Bio- and Neuro- Engineering, Geneva, 1202, Switzerland.

15 <sup>f</sup>Division of Neurorehabilitation, Department of Clinical Neurosciences, University Hospital Geneva,  
16 Geneva, Switzerland

17 <sup>g</sup>Laboratory of Cognitive Neurorehabilitation, Department of Clinical Neurosciences, Medical School,  
18 University of Geneva, Geneva, Switzerland

19 \*Equally contributing authors

## 20 **Corresponding author**

21 Christian Giang: [christian.giang@epfl.ch](mailto:christian.giang@epfl.ch)

## 22 **Co-authors emails**

23 Elvira Pirondini: [Elvira.Pirondini@unige.ch](mailto:Elvira.Pirondini@unige.ch), Nawal Kinany: [nawal.kinany@epfl.ch](mailto:nawal.kinany@epfl.ch), Camilla Pierella:  
24 [camilla.pierella@epfl.ch](mailto:camilla.pierella@epfl.ch), Alessandro Panarese: [a.panarese@santannapisa.it](mailto:a.panarese@santannapisa.it), Martina Coscia:  
25 [martina.coscia@wysscenter.ch](mailto:martina.coscia@wysscenter.ch), Jenifer Miehlsbradt: [jenifer.miehlsbradt@epfl.ch](mailto:jenifer.miehlsbradt@epfl.ch), Cécile Magnin:  
26 [Cecile.Magnin@hcuge.ch](mailto:Cecile.Magnin@hcuge.ch), Pierre Nicolo: [Pierre.Nicolo@hcuge.ch](mailto:Pierre.Nicolo@hcuge.ch), Adrian Guggisberg:  
27 [Adrian.Guggisberg@hcuge.ch](mailto:Adrian.Guggisberg@hcuge.ch), Silvestro Micera: [silvestro.micera@epfl.ch](mailto:silvestro.micera@epfl.ch)

28 **Abstract.** *Background:* In the past years, robotic systems have become increasingly popular  
29 in both upper and lower limb rehabilitation. Nevertheless, clinical studies have so far not been  
30 able to confirm superior efficacy of robotic therapy over conventional methods. The  
31 personalization of robot-aided therapy according to the patients' individual motor deficits has  
32 been suggested as a pivotal step to improve the clinical outcome of such approaches.  
33 *Methods:* Here, we present a model-based approach to personalize robot-aided rehabilitation  
34 therapy within training sessions. The proposed method combines the information from  
35 different motor performance measures recorded from the robot to continuously estimate  
36 patients' motor improvement for a series of point-to-point reaching movements in different  
37 directions and comprises a personalization routine to automatically adapt the rehabilitation  
38 training. We engineered our approach using an upper limb exoskeleton and tested it with  
39 seventeen healthy subjects, who underwent a motor-adaptation paradigm, and two subacute  
40 stroke patients, exhibiting different degrees of motor impairment, who participated in a pilot  
41 test. *Results:* The experiments illustrated the model's capability to differentiate distinct motor  
42 improvement progressions among subjects and subtasks. The model suggested personalized  
43 training schedules based on motor improvement estimations for each movement in different  
44 directions. Patients' motor performances were retained when training movements were  
45 reintroduced at a later stage. *Conclusions:* Our results demonstrated the feasibility of the  
46 proposed model-based approach for the personalization of robot-aided rehabilitation therapy.  
47 The pilot test with two subacute stroke patients further supported our approach, while  
48 providing auspicious results for the applicability in clinical settings.

49 *Trial registration:* This study is registered in ClinicalTrials.gov (NCT02770300, registered 30  
50 March 2016, <https://clinicaltrials.gov/ct2/show/NCT02770300>).

51 **Keywords:** Personalized therapy, rehabilitation robotics, stroke rehabilitation,

## 52 **1 Background**

53 With the increase of life expectancy, it is estimated that stroke related impairments will be  
54 ranked fourth most important cause of disability in western countries in 2030 [1]. With about  
55 80% of stroke survivors experiencing significant motor impairment [2], stroke rehabilitation  
56 represents a major challenge. Despite early rehabilitative interventions, 55% to 75% of the  
57 patients still suffer from upper limb impairments in the chronic state of the injury [3–5]. The  
58 recovery of reaching and grasping movements is therefore a crucial therapeutic goal in stroke  
59 rehabilitation [6].

60 Post-stroke rehabilitation usually relies on task-oriented repetitive movements that help  
61 improving motor function and training new control strategies. In this regard, the amount of  
62 goal-directed and challenging practice, rather than daily intensity alone, seems to be the most  
63 effective factor in neurorehabilitation [7]. In the last two decades, robot-aided motor training  
64 has shown potential for the recovery of lost motor abilities in upper limbs after stroke [8–10].  
65 While providing intense and highly repeatable motor training, robotic devices also offer  
66 means to control and quantify movement performances. Despite this undeniable potential,  
67 controlled clinical trials have so far not been able to confirm whether robotic therapy is more  
68 effective than conventional methods in restoring motor abilities [11, 12]. It has been argued  
69 that this might be related to saturation effects and a lack of automatic methods to promptly  
70 detect them [13].

71 The automatic and personalized adaptation of the rehabilitation training has been suggested as  
72 a pivotal step to improve the outcome of robot-aided rehabilitation and the clinical relevance  
73 of such solutions [14]. As a matter of fact, motor learning is known to be maximized when the  
74 difficulty level of the training task matches the patient’s level of ability [15]. Recent advances  
75 in the field of personalized robotic rehabilitation have therefore focused on the design of  
76 customized training protocols, including individualized selection of upper limb movements

77 [16]. Different measures have been used to assess the patient's "status" during training (i.e.,  
78 motor performance, engagement, etc.) in order to adjust the proposed tasks accordingly.  
79 Kinematic performance measures, such as movement accuracy, smoothness, speed, inter-joint  
80 coordination, range of motion and stiffness [17–23], game-related statistics [13, 24], measures  
81 of muscle activity [17], or the combination of kinematic and psychophysiological  
82 measurements [25–27] have been among the measures used for the design of patient-tailored  
83 training protocols. However, those approaches either focused on a single performance  
84 measure describing a specific aspect of rehabilitation or used multiple measures but lacked the  
85 ability to meaningfully synthesize the information from all these variables. Integrating this  
86 information into a single measure, yet representative of the patient's multidimensional  
87 rehabilitation response, would provide a straightforward method to track the multifaceted  
88 progress of the patient and trigger task adaptation while enormously simplifying the design of  
89 personalized rehabilitation training.

90 An interesting approach to address this issue was presented in the work of Panarese et al. [28].  
91 The authors used a state-space model to merge the information from different kinematic  
92 measures and, in this way, estimated the motor improvement of chronic stroke patients  
93 exercising with a planar robotic device for upper limb rehabilitation. Similar methodologies  
94 have previously allowed to successfully characterize cognitive learning in animals [29, 30].  
95 The results of Panarese et al. emphasized the potential of extending such approaches to the  
96 context of neurorehabilitation. In their study, the authors showed that the devised model was  
97 capable of mimicking decision rules applied by physical therapists regarding the adaptation of  
98 the task difficulty. In some cases, the model even appeared to be faster than the therapists in  
99 detecting when the patients' motor performance had reached a plateau and when more  
100 challenging tasks should have been proposed.

101 In this work, we built on these results to implement a method able to continuously detect

102 patient's motor improvement and adapt the training task for three-dimensional movements  
103 using an upper limb exoskeleton. Indeed, most of the aforementioned adaptive approaches  
104 were restricted to planar workspaces, hindering their applications to functional movements  
105 exploring three-dimensional workspaces, which better resemble those performed during daily  
106 life activities. Evaluating and estimating motor improvement is particularly compelling in  
107 three-dimensional training workspaces, where the visual evaluation of motor performance  
108 becomes more challenging. Under these circumstances, a method able to autonomously  
109 estimate patient training progress, in particular for movements in different directions, could  
110 provide fundamental support to the therapists, enabling them to shift their focus from visual  
111 inspection of the movements performed to other important aspects of training. In this study,  
112 we also aimed at a continuous implementation of the motor improvement estimation and the  
113 personalization routine. Indeed, the immediate task adaptation within training sessions could  
114 not only increase patients' engagement, but also foster their attention control, possibly leading  
115 to improved reaching performances [31].

116 In order to enable the use of such methods for clinical applications, it is first necessary to  
117 validate their feasibility and safety under controlled experimental conditions. We, therefore,  
118 devised an experiment to test our approach in a group of healthy subjects. In order to mimic  
119 the motor improvement observed in stroke patients, we applied a visual manipulation to the  
120 training environment. Previous studies on visually manipulated motor tasks showed that most  
121 people could cope with similar manipulations after training [32–36]. Accordingly, we  
122 hypothesized that performances would drop after the introduction of the inverted visual  
123 feedback (i.e., movements would become slower and less smooth), but would then gradually  
124 improve and eventually reach a plateau - with temporal dynamics resembling the ones  
125 occurring in robot-aided rehabilitation of stroke patients [28, 37, 38]. Using this setup, we  
126 tested whether our model was capable of tracking individual motor improvements induced by

127 motor adaptation, and whether it was able to personalize the training by identifying  
128 “recovered” (i.e., adapted) movements in real-time. To provide further evidence about the  
129 feasibility and clinical usability of the presented approach, we finally performed a pilot test  
130 with two subacute stroke patients. The test was conducted in the framework of robot-aided  
131 upper-limb rehabilitation training for subacute stroke patients.

## 132 **2 Results**

### 133 **2.1 Experimental validation with healthy participants**

134 We first experimentally validated our model in a group of 17 healthy participants. Using the  
135 robotic upper limb exoskeleton ALEx [39, 40], we designed a three-dimensional point-to-  
136 point reaching task (Fig. 1a-b), a training exercise commonly used in robotic rehabilitation  
137 therapy [41–43]. In order to challenge the subjects and make them adapt to a new motor  
138 control scheme with temporal dynamics similar to those observed in robot-aided rehabilitation  
139 of stroke patients, the visual feedback was manipulated during five inversion blocks  $B_{1-5}$  (Fig.  
140 1c, see Section 5.6.1). Under these circumstances, we tested whether our model was capable  
141 of continuously tracking MI (in this case induced by motor adaptation) and whether our  
142 implementation could personalize the training by identifying adapted movements (i.e.,  
143 movements with performance comparable to the non-inverted condition) and by replacing  
144 them with more difficult ones.

145 *Figure 1 around here*

#### 146 **2.1.1 Task adaptation at subject level**

147 Despite a general improvement for all participants, the subjects differed considerably in their  
148 adaptation speed, as quantified by the number of new targets introduced during the inversion  
149 blocks  $B_{1-5}$ . We identified two groups using a median cut and found that the number of new  
150 targets for fast adapters ( $n = 9$ ,  $7.7 \pm 1.2$  new targets, mean  $\pm$  std over subjects) and slow

151 adapters ( $n = 8$ ,  $2.6 \pm 2.0$  new targets) was significantly different ( $p < 0.001$ ).

152 Interestingly, the two groups already showed differences in performance during the initial  
153 assessment  $A_{I,1-3}$  (Fig. 2a-c). Specifically, the values for MV were significantly higher ( $p <$   
154  $0.001$ ) for the slow adapters ( $0.171 \pm 0.041$  m/s, mean  $\pm$  sem over subjects) in comparison to the  
155 fast adapters ( $0.159 \pm 0.040$  m/s). In contrast, the values for SAL were significantly lower ( $p <$   
156  $0.001$ ) for the slow adapters ( $-3.134 \pm 0.715$ ) compared to the fast adapters ( $-2.807 \pm 0.596$ ). For  
157 the rate of SUCC no significant difference ( $p = 0.06$ ) was found between slow ( $96.5 \pm 1.1$  %)  
158 and fast ( $100 \pm 0.0$  %) adapters.

159 *Figure 2 around here*

160 As expected, the performance measures worsened for both groups after the introduction of the  
161 visual manipulation. However, the drop was remarkably smaller for the fast adapters: between  
162 the last run of the initial assessment  $A_{I,3}$  and the first run of the inverted block  $B_1$ , the values  
163 for MV worsened by  $0.048$  m/s ( $-29\%$  compared to  $A_{I,3}$ ) for the fast adapters and by  $0.074$   
164 m/s ( $-41\%$ ) for slow adapters. The values for SAL worsened by  $1.346$  ( $-50\%$ ) for the fast  
165 adapters and by  $4.802$  ( $-157\%$ ) for the slow adapters. The rate of SUCC worsened by  $57\%$  for  
166 the fast adapters and  $87\%$  for the slow adapters. A two-way ANOVA illustrated the different  
167 impact of the introduced inversion on each group measured by MV ( $F_{1,421} = 10.62$ ,  $p = 0.001$ ),  
168 SAL ( $F_{1,421} = 112.31$ ,  $p < 0.001$ ) and rate of SUCC ( $F_{1,421} = 30.38$ ,  $p < 0.001$ ).

169 Both groups gradually improved from  $B_1$  to  $B_5$ , although they did not reach their initial motor  
170 performances (i.e., performances during  $A_{I,1-3}$ ). A comparison between the last run of  $B_5$  and  
171 the last run of the initial assessment  $A_{I,3}$  showed that the fast adapters were more successful in  
172 restoring their initial performances: compared to their baseline level, MV was lowered by  
173  $0.014$  m/s ( $-9\%$  compared to  $A_{I,3}$ ) for the fast adapters and by  $0.051$  m/s ( $-30\%$ ) for slow  
174 adapters). The values for SAL were lowered by  $0.581$  ( $-22\%$ ) for the fast adapters and by

175 0.783 (-25%) for the slow adapters. The rate of SUCC was lowered by 18% for the fast  
176 adapters and by 45% for the slow adapters. During the entire experiment, the fast adapters  
177 outperformed the slow adapters and reached better final values for all performance measures,  
178 (+0.024 m/s for MV, +0.583 for SAL and +31% for rate of SUCC for the fast adapters at the  
179 last run of B<sub>5</sub>).

180 These results illustrate that the improvements induced by motor adaptation exhibited subject-  
181 specific dynamics, prompting the need for a model capable of differentiating between time  
182 courses of MI at subject level. We observed a coherency between the chosen performance  
183 measures and the adaptation speed quantified by the number of new training targets  
184 introduced. Fast adapters exhibited remarkably better performance compared to the slow  
185 adapters and they were thus introduced to considerably more training targets.

### 186 **2.1.2 Task adaptation at subtask level**

187 In addition to the ability to differentiate MI for different subjects, we were interested in  
188 assessing whether the model was able to monitor MI at subtask level in a three-dimensional  
189 environment. Therefore, we evaluated which initial training targets were replaced by the  
190 algorithm during the inversion blocks and when this replacement occurred (Fig. 2d). The  
191 insertion of new targets did not start before B<sub>3</sub>, as in B<sub>1-2</sub> the amount of data for each training  
192 target was not sufficient to obtain proper MI estimations (see section 5.1). As hypothesized in  
193 the experimental design, movements towards the off-axis targets (2, 4, 6, 8, 11, 14, 15, 16, 17  
194 and 18, Fig. 1b) seemed to be more difficult: on average, the algorithm replaced these targets  
195 for 13% of the slow adapters and for 77% of the fast adapters. The on-axis targets (1, 3, 5, 7,  
196 10 and 13), instead, were replaced for 38% of the slow adapters and 87% of the fast adapters.  
197 However, we also observed differences within the on-axis targets: on average, targets 3, 5 and  
198 13 were replaced for 13% of the slow adapters and for 74% of the fast adapters, while the  
199 replacement for targets 1, 7 and 10 was achieved by 63% of the slow adapters and by 100% of



200 the fast adapters. Following this analysis, we identified the subsets of easy (1, 7 and 10) and  
201 difficult (3, 5, 13 and off-axis) targets. Interestingly, the results suggested that despite the  
202 differences in the overall performance, the subsets of easy and difficult targets appeared to be  
203 similar for both groups. Nevertheless, we observed an earlier replacement of the easy targets  
204 for the fast adapters: 56% of the easy targets were replaced in B<sub>3</sub> (4% for slow adapters), 33%  
205 were replaced in B<sub>4</sub> (38% for slow adapters), and 11% were replaced in B<sub>5</sub> (21% for slow  
206 adapters). In contrast, for the difficult targets, the fast adapters also needed more time to  
207 achieve a replacement (if they were replaced eventually): 26% of the difficult targets were  
208 replaced in B<sub>3</sub> (3% for slow adapters), 35% were replaced in B<sub>4</sub> (5% for slow adapters) and  
209 14% were replaced in B<sub>5</sub> (5% for slow adapters).

210 To illustrate the behavior of individual participants at subtask level, we present the data of one  
211 exemplary subject from each group for the movements towards the same two targets (Fig. 3).  
212 We selected one target from the subset of the easy (target 10) and one target from the subset  
213 of the difficult (target 13) targets. The examples illustrate the different adaptation rates  
214 observed between subjects and targets. For the easy target, the performance measures for the  
215 fast adapter quickly improved and approached a plateau. The slow adapter, instead, showed  
216 difficulties until the fourth repetition, reflected particularly by SAL and SUCC. Nonetheless,  
217 starting from the fifth repetition, he/she also managed to adapt the movements to the distorted  
218 visual feedback and finally reached the conditions for the target replacement at the twelfth  
219 repetition. The difficult target, instead, appeared to be more challenging for both subjects. For  
220 this target, the fast adapter showed an improvement in all performance measures only after the  
221 tenth repetition and finally reached the conditions for the target replacement after eighteen  
222 repetitions. In contrast, the slow adapter did not manage to satisfy the conditions for a  
223 replacement. Despite a trend of improvement, the motor performance was never sufficient to  
224 trigger a replacement of the target.

225

*Figure 3 around here*

226 These examples highlight the capability of the model to continuously capture individual time  
227 courses of improvement at subtask level. Furthermore, the results emphasized that the  
228 proposed model could detect saturation in motor performance and trigger actions regarding  
229 task difficulty in a well-timed manner.

## 230 **2.2 Pilot test**

231 To provide further evidence about the feasibility of the presented approach, we finally  
232 performed a pilot test with two subacute stroke patients, who completed four weeks of  
233 personalized robot-aided training in addition to standard rehabilitation therapy (Fig. 1d, see  
234 Section 5.5 for details). During the training, the set of targets was automatically adapted based  
235 on a continuous evaluation of the MI estimates for each training target.

236 Based on the initial assessment of their FMA-UE scores, we observed a remarkable difference  
237 in the degree of motor impairment of patient P01 (22 points at  $A_{I,2}$ , Fig. 4a) compared to  
238 patient P02 (59 points at  $A_{I,2}$ ). This difference was reflected by the number of movements  
239 (nMov) performed in the training session, which was notably lower for P01 (31 movements  
240 compared to 69 movements for P02 at  $A_{I,2}$ ). The different degrees of initial impairment  
241 allowed us to evaluate the feasibility of our approach for two patients exhibiting disparate  
242 initial motor abilities.

243 Following the training, both patients showed improvements for MV, SAL, and SUCC. When  
244 comparing the values right before ( $A_{I,2}$ ) and right after ( $A_{F,1}$ ) the treatment sessions, we  
245 observed that patient P01 improved MV (+0.378 m/s), SAL (+1.60) and rate of SUCC  
246 (+22%). In comparison, improvements for patient P02 were lower for MV (+0.293 m/s),  
247 slightly higher for SAL (+1.77) and remarkably lower for SUCC (+1.6%). The latter can be  
248 explained by the fact that the values for SUCC for patient P02 already started at a very high

249 level (98% at  $A_{I,2}$ ), leaving smaller room for improvement. Interestingly, both patients  
250 managed to retain or even improved their performance in the follow-up assessment ( $A_{F,2}$ ) four  
251 weeks after completion of the training. The only exception was observed for patient P01, who  
252 slightly worsened in SUCC between  $A_{F,1}$  and  $A_{F,2}$ . However, this difference did not appear to  
253 be statistically significant ( $p = 0.61$ ). Along with the improvements of the performance  
254 measures, we also observed higher FMA-UE scores for both patients following the training.  
255 In that respect, we also observed a lower increase for patient P02 (+3 points) compared to  
256 patient P01 (+8 points) between  $A_{I,2}$  and  $A_{F,1}$ . Interestingly, both patients further improved  
257 their FMA-UE scores when assessed in the follow-up session  $A_{F,2}$ . Finally, we also observed  
258 an increase in the number of performed movements per session (nMov) for both patients. As  
259 for this measurement, instead, patient P02 (+40 movements at  $A_{F,1}$  and +76 movements at  
260  $A_{F,2}$  compared to  $A_{I,2}$ ) improved more than patient P01 (+23 movements at  $A_{F,1}$  and  $A_{F,2}$   
261 compared to  $A_{I,2}$ ).

262 *Figure 4 around here*

263 Both patients progressed during the rehabilitation training and eventually achieved a  
264 replacement of all eighteen training targets. However, the temporal dynamics of these  
265 replacements appeared to be strongly different for each patient (Fig. 4b). In line with the  
266 lower degree of motor impairments observed from the performance measures and the FMA-  
267 UE scores, patient P02 achieved a replacement of all training targets after only two training  
268 sessions. Patient P01, instead, needed considerably more time to achieve the replacement of  
269 all eighteen targets. While some of the initial training targets (i.e. targets 9 and 12) were  
270 already replaced after two treatment sessions, other targets (i.e. targets 1, 7 and 15) needed  
271 more than 4 training sessions to trigger a replacement. It was only after eleven treatment  
272 sessions that all eighteen training targets were presented to patient P01. These observations  
273 emphasized the ability of our model to differentiate between both subject- and subtask-

274 specific time courses of motor improvement, also in a real clinical setting. The examples  
275 illustrate how the model adapted the training schedules according to the patients' individual  
276 abilities, granting patient P01 enough time to practice the movements, and at the same time,  
277 responding to the fast recovery of patient P02 by continuously introducing new training  
278 targets.

279 Upon completion of the full set of training targets (i.e., when all targets had been replaced at  
280 least once), the therapy was carried on by reintroducing all targets and presenting them  
281 alternatingly in the order in which they were replaced. This allowed us assessing whether the  
282 patients' performance was retained once a training target was reintroduced, so as to validate  
283 that the replacements orchestrated by the algorithm had occurred when the movements  
284 towards the targets had actually recovered. In order to do so, we compared the mean values  
285 for MV, SAL, and SUCC from the last four repetitions of a movement before a target was  
286 replaced by the algorithm with the mean values of the four repetitions of the same movement  
287 after the first reinsertion as a training target (Fig. 4c). Both values are presented relatively to  
288 the mean values obtained from the first initial four repetitions of the movements towards a  
289 training target. The overall analysis for all eighteen targets showed that compared to the initial  
290 movements towards the targets, almost all values for the three performance measures were  
291 higher (MV by +8% for P01 and by +12% for P02, SAL by +3% (+10%) and SUCC by +10%  
292 (+0%)) right before the targets were replaced by the algorithm. Moreover, both patients  
293 retained or even improved their performance for a movement when the corresponding training  
294 target was reintroduced at a later stage. For both patients, we found no significant difference  
295 ( $p > 0.077$ ) for the values of all three performance measures between the two time points (i.e.,  
296 before replacement and after reinsertion). These results illustrate that the algorithm only  
297 replaced training targets when motor performance had stably improved. More importantly,  
298 both patients have retained these improvements when the training targets were reintroduced at

299 a later stage, suggesting that the timing of the replacement was appropriate.

### 300 **3 Discussion**

301 In this study, we presented and validated a model-based approach for the personalization of  
302 robotic rehabilitation training based on motor performance during three-dimensional training  
303 tasks. Capitalizing on the enhanced potential for plasticity in the early stage after the injury  
304 [44, 45], the model was designed to allow estimation of motor improvement (MI) in subacute  
305 stroke patients. A first experimental validation in healthy subjects demonstrated the ability of  
306 our model to capture MI linked to visual motor adaptation. The results were further validated  
307 by a clinical pilot test with two subacute stroke patients, in which motor recovery was tracked  
308 and harnessed by our personalization method.

#### 309 **3.1 Motor improvement model for 3D reaching tasks**

310 One of the pivotal aspects underlying the development of a personalized rehabilitation  
311 training is the definition of performance measures that can correctly capture the different  
312 aspects of motor recovery, as well as their specific dynamics. Three performance measures  
313 were selected based on previous studies [28, 46] and used to devise a state-space model for  
314 MI estimation: movement velocity (MV), spectral arc length (SAL), and robot assistance  
315 dependency (SUCC). In past studies, the selected measures have been shown to correlate with  
316 clinical scores [47] and they have been linked to distinct post-stroke deficits and mechanisms  
317 of recovery [48, 49]. Specifically, the percentage of accomplished tasks was mostly associated  
318 to paresis (i.e., the decreased ability to volitionally modulate motor units activation [50]),  
319 whereas movement speed and smoothness were related to an abnormal muscle tone [48]. We  
320 therefore hypothesized that considering a combination of these measures was necessary to  
321 obtain a comprehensive assessment of the patient's rehabilitative status. As such, we aimed to  
322 design a model capable of integrating the information coming from these multiple variables

323 into a single motor performance measure, that could i) allow a better tracking of the patient's  
324 rehabilitation progress, and ii) simplify the design of an automatic and personalized training  
325 protocol, therefore possibly enhancing the efficacy of the robot-aided rehabilitation training.

326 Using the robotic upper limb exoskeleton ALE<sub>x</sub> [39, 40], we designed a three-dimensional  
327 point-to-point reaching task, a training exercise commonly used in robotic rehabilitation  
328 therapy [41–43]. The movement amplitude was selected to allow the exploration of a  
329 functional workspace, while movement directions were chosen to elicit independent and  
330 synergistic motion of shoulder and elbow, capitalizing on the advantages provided by robotic  
331 exoskeleton devices [51]. Such design not only allowed the users to explore an extensive  
332 workspace, but also provided a way to easily assess their performance for the different regions  
333 of the workspace (i.e., for different subtasks, represented by the movements towards the  
334 different targets). The reaching task was displayed on a screen mounted in front of the  
335 participants and visual feedback was provided by means of a cursor mapping the position of  
336 the exoskeleton's handle to the screen, an important aspect to avoid compensatory strategies  
337 [13]. The choice of a 2D screen was justified by the typically advanced age of post-stroke  
338 patients, who are usually not familiar and, therefore, often discomforted by 3D immersive  
339 reality. In order to preserve the depth perception, the dimension of the target spheres was  
340 modified in accordance with their position in the 3D space. Preliminary data from a group of  
341 age-matched healthy subjects (see *Supplementary*) showed that performance measures were  
342 not different for targets on the depth axes, confirming that the depth could be properly  
343 perceived by the users.

### 344 **3.2 Adaptation to visually manipulated reaching tasks in 3D**

345 We first sought to validate the model's ability to continuously track MI and dynamically  
346 adjust the training task under controlled conditions. To this end, we presented a motor  
347 adaptation task to a group of seventeen healthy subjects. In order to mimic the motor deficits

348 observed in stroke patients, we introduced a manipulation of the visual feedback, by inverting  
349 the directions of the 3D environment. While the physiological mechanisms underlying motor  
350 adaptation and motor recovery are most likely not equivalent, the main objective of this  
351 experimental design was merely to obtain an adaptation curve that resembles post-stroke  
352 motor recovery, on which we could validate the efficacy of our model. Our results indeed  
353 illustrated that motor adaptation in healthy subjects and motor recovery in stroke patients  
354 exhibited similar temporal dynamics.

355 During the experiments, the MI model tracked when a movement towards a target was  
356 performed efficiently despite the visual perturbation, and subsequently adjusted the training  
357 by replacing this target with a more difficult one from the training queue. Interestingly, we  
358 observed that the number of new training targets inserted strongly differed across participants,  
359 pointing out varying adaptation speeds. This result was not expected *a priori*, but it emerged  
360 as an unforeseen opportunity to highlight the model's capability to differentiate individual  
361 motor adaptation rates. Based on the number of new inserted training targets, we divided the  
362 healthy population into two separate clusters: fast and slow adapters. The analysis on the  
363 performance measures showed that the fast adapters learned to cope with the manipulated  
364 environment very quickly, while the slow adapters needed considerably more time to reach  
365 similar performances. Interestingly, the two groups already showed differences in motor  
366 performances during the initial assessment. When the visual feedback was manipulated, the  
367 slow adapters presented a strongly reduced speed and motion smoothness. This was  
368 particularly the case earlier before the use of the adaptive algorithm and we, therefore, believe  
369 that the latter did not have an influence on the participants' performance. The MI model,  
370 instead, was able to capture these individual performance differences at subtask level and  
371 coherently introduced new training subtasks in a well-timed manner, i.e., targets were  
372 replaced when subjects reached a performance plateau. The advantages of monitoring motor

373 improvement at subtask level were supported by additional post-hoc analyses (see  
374 *Supplementary material*). The analyses illustrated that if motor improvements were estimated  
375 for the reaching task as a whole (i.e., combining the recorded data for movements in all  
376 directions), improvements for individual subtasks would have been obscured by inferior  
377 performances of other, more difficult, subtasks. Moreover, the detection of performance  
378 plateaus would not correspond to the actual performances for any subtask. As a result, some  
379 subtasks would be kept too long, while others would be replaced too soon, potentially leading  
380 to a less efficient training schedule. For instance, the overall MI estimate based on the first 80  
381 repetitions of the slow adapter suggests a performance plateau already after 39 repetitions  
382 (which corresponds to approximately 5 repetitions for each subtask). However, when looking  
383 at the performance measures of this subject for target 13 separately, it is clear that a  
384 replacement of this target after 5 repetitions would have been premature. We therefore believe  
385 that this analysis further supports our approach to specifically consider MI estimation at  
386 subtask level.

387 As hypothesized in the experimental design, off-axis targets were replaced less often than on-  
388 axis targets and they, thus, seemed to be more difficult. However, the results showed that  
389 there were also remarkable performance differences among the on-axis targets. An analysis on  
390 the replaced training targets demonstrated that the subsets of easy (1, 7 and 10) and difficult  
391 (3, 5, 13 and off-axis) targets appeared to be similar for both types of adapters: easy targets  
392 were mostly replaced earlier and more frequently than the difficult ones. It could be that the  
393 medial and proximal movements towards targets 7 and 10 tended to be easier for the  
394 participants. However, since these tendencies were not observed in the patients or the healthy  
395 subjects involved in the preliminary study (see *Supplementary material*), we presume that the  
396 performance differences for the on-axis targets could be linked to the visually manipulated  
397 environment. Previous studies have investigated visual manipulation in planar reaching



398 movements and suggested that the adaptation to such manipulations involves a complex  
399 mixture of implicit and cognitive processes [33, 52]. However, further research would be  
400 necessary to examine these phenomena in three-dimensional reaching movements. As a  
401 matter of fact, existing literature covering this area is still relatively sparse. In this context, it  
402 would be interesting to determine why the reaching movements towards some on-axis targets  
403 appeared to be more challenging in the inverted environment, independent from the individual  
404 adaptation speed of the subjects.

405 Finally, we would also like to raise the question of psychological implications resulting from  
406 the automated training adaption. From qualitative observations made during the experiments  
407 with the healthy subjects, we noticed that many participants showed increased motivation and  
408 verbalized satisfaction when new training targets were introduced. Motivation is known to be  
409 a crucial factor in rehabilitation and finding ways to maintain and improve it has always been  
410 a matter of interest [53–55]. With regard to this issue, it seems like the automated character of  
411 our approach, enabling dynamic and well-timed task adaptation, may have positive impacts  
412 on training engagement. Transferring this benefit to the rehabilitation program of patients may  
413 promote training motivation and hence potentially improve the clinical outcome of robot-  
414 aided rehabilitation trainings.

### 415 **3.3 Personalization of rehabilitation therapy**

416 The potential of our implementation was finally evaluated in a clinical pilot test with two  
417 subacute stroke patients, who completed four weeks of robot-aided rehabilitation training  
418 following our adaptive approach.

419 The results obtained from these two patients suggested that in general, the selected  
420 performance measures (MV, SAL and SUCC) appeared to be suitable for the use with the  
421 presented motor improvement model and the temporal dynamics appeared to be coherent with

422 the chosen probability models and with results from previous work [49]. We observed  
423 improvements for all three performance measures following the training. Nevertheless, some  
424 tuning of the parameters could be considered to further enhance the efficacy of the motor  
425 improvement model. For instance, we observed that the patient with a lower degree of initial  
426 impairments (P02) barely made use of the robotic assistance provided by the exoskeleton,  
427 leading to almost no variance in the variable SUCC. In this regard, future studies may explore  
428 other performance measures and models, such as the ones proposed by Panarese et al. [28,  
429 49], to achieve a more exhaustive evaluation of the patients' status.

430 Based on the devised method, the training of the two patients following the personalized  
431 rehabilitation protocol was continuously monitored and the point-to-point reaching task was  
432 adapted in real-time to match their level of ability. The analysis showed that targets were  
433 indeed replaced by the model at appropriate moments, i.e., when the patients' performance  
434 had improved and started to saturate. Indeed, it could be argued that a replacement of a  
435 subtask occurring too soon would have led to degraded motor performances in further  
436 evaluations. However, the results demonstrated that motor performances of both patients were  
437 retained when targets were reintroduced, indicating that the estimated recovery was preserved.  
438 Nevertheless, other methods for training scheduling could be introduced to further optimize  
439 the training progression. Indeed, previous work has suggested that effective scheduling of  
440 multitask motor learning should be based on prediction of long-term gains rather than on  
441 current performance changes [56]. Along these lines, we have implemented the time window  
442 of the last four repetitions, which are always taken into account for the evaluation of motor  
443 performance. However, it should be acknowledged that other, more sophisticated, methods to  
444 adapt the schedules may lead to higher gains in rehabilitation and are therefore worth  
445 exploring. For instance, task difficulty could be increased by introducing new subtasks  
446 depending on more complex movements within the same workspace, in order to exploit

447 generalization effects [57, 58]. Another possible approach could be a semi-automatic  
448 implementation of the personalization, where the physical therapists remains in charge of the  
449 task adaptation, in order to benefit from their expertise, while in parallel harnessing the real-  
450 time MI estimates provided by the model as a decision support. Such solutions could further  
451 improve engagement and enhance the rehabilitative treatment by providing training tasks  
452 specifically adapted to the ability level of the patient.

453 As a way to measure the clinical outcome of the rehabilitative interventions, the patients  
454 completed the Fugl-Meyer assessment for upper extremities in all initial and final assessment  
455 sessions. When comparing the scores of the patients between the second initial assessment  
456  $A_{I,2}$  and the first final assessment  $A_{F,1}$ , we found that both patient P01 (+8 points) and patient  
457 P02 (+3 points) improved. Considering the scores at the follow-up session,  $A_{F,2}$ , four weeks  
458 after completion of the training, this improvement was further sustained for both patients (+12  
459 points for P01 and +6 points for P02). In addition to this gain in FMA-UE scores, the  
460 improvement of motor performance, along with its subsequent retention at target reinsertion,  
461 are promising indications for the usability and efficacy of the presented approach in clinical  
462 settings. Nevertheless, it is also well known that subacute patients often report motor  
463 improvements even with limited training [59]. Therefore, it cannot be presumed that  
464 improvements were merely elicited by the robotic rehabilitation trainings. However, several  
465 pieces of evidence suggested that the period immediately after the lesion, normally  
466 characterized by spontaneous neurological recovery, represents the critical time window in  
467 which the delivery of high dose and intense neurorehabilitation can elicit crucial  
468 improvements in functional tasks [60, 61]. Therefore, more and more robot-aided  
469 rehabilitation trainings should be targeting subacute stroke populations. In this context, our  
470 results illustrate the feasibility of using a personalization method to continuously monitor the  
471 status of both mild and severely impaired post-stroke patients and to automatically adapt their

472 motor retraining within practice sessions. The latter might be particularly pivotal in the  
473 context of rehabilitation training for subacute stroke patients. In contrast to chronic patients,  
474 this population often shows potential for quick recovery [49], calling for prompt training  
475 adjustments in order to continuously challenge their neuromuscular system.

476 Nevertheless, further studies including larger cohorts of participants would be necessary to  
477 draw meaningful conclusions about the clinical relevance of the presented approach. In this  
478 context, it would be particularly interesting to compare the clinical outcomes of the  
479 personalized approach presented in this study with non-adaptive robotic or conventional  
480 rehabilitation trainings. Indeed, previous work has suggested that pseudo-random scheduling  
481 of multiple tasks may be almost as effective as adaptive scheduling approaches [56]. To  
482 demonstrate clinical relevance, it is therefore crucial to assess the efficacy of the presented  
483 approach in large clinical trials, focusing their activity on the comparison of adaptive and non-  
484 adaptive schedules. In this context, the results obtained from this work may provide a useful  
485 basis for the design and implementation of such clinical studies.

## 486 **4 Conclusions**

487 In this work, we presented a model-based approach to personalize robot-aided rehabilitation  
488 therapy within rehabilitation sessions. The feasibility of this approach was validated in  
489 experiments with seventeen healthy subjects and a pilot test with two subacute stroke patients  
490 providing promising results. However, due to the limited sample size, larger studies would be  
491 needed to demonstrate clinical relevance of the presented approach. While we implemented  
492 the proposed method for the use in upper limb rehabilitation of stroke patients, the usage is  
493 certainly not limited to such applications. The presented model can be adapted for the use  
494 with other robotic rehabilitation devices and training tasks, exploiting different performance  
495 measures and/or different observation equations. The real-time functionality and the

496 identification of subject-specific abilities at subtask level could enhance robot-aided  
497 rehabilitation training, making it more purposive and efficient for the patients.

## 498 **5 Methods**

499 Based on the work of Panarese et al. [28], we developed a model to continuously estimate  
500 motor improvement (MI) in three-dimensional workspaces using kinematic performance  
501 measures. We then designed a personalization routine, which automatically adapts the  
502 difficulty of the rehabilitative motor task (i.e., a point-to-point reaching task) based on the MI  
503 estimates. Both the MI model and the personalization routine were integrated in the control  
504 algorithm of an upper-limb exoskeleton and tested with a group of 17 healthy participants.  
505 The presented approach was then tested with two subacute stroke patients.

### 506 **5.1 Motor improvement model**

507 In order to continuously track patients' MI at subtask level (i.e., for a series of point-to-point  
508 reaching movements in different directions), we used a state-space model. MI was modelled  
509 as a random walk:

$$MI_k = MI_{k-1} + \epsilon_k \quad (1)$$

510 where  $k$  are the different repetitions for a movement direction and  $\epsilon_k$  are independent  
511 Gaussian random variables with zero mean and variance  $\sigma_\epsilon^2$ . A set of observation equations  
512  $z_{j,k}$  was defined in order to estimate MI. These equations related MI to continuous  
513 performance measures  $r_j$ , which were computed from kinematic recordings provided by the  
514 robotic device (see section 5.2 for details on the performance measures). The continuous  
515 variables  $r_j$  (with  $j = 1, \dots, J$  representing the different performance measures) were defined  
516 by the log-linear probability model

$$z_{j,k} = \log(r_{j,k}) = \alpha_j + \beta_j MI_k + \delta_{j,k} \quad (2)$$

517 where  $\delta_{j,k}$  are independent Gaussian random variables with zero mean and variance  $\sigma_{\delta,j}^2$ . The  
518 use of log-linear models allowed capturing rapid increases (or decreases) of the performance  
519 measures during the training, as well as the expected convergence towards subject-specific  
520 upper (or lower) bounds at the end of the training. The suitability of such probability models  
521 for motor performance measures in stroke patients was previously demonstrated [28, 49].  
522 Similarly, an observation equation for a discrete performance measure  $n_k$  was defined. The  
523 binary discrete variable  $n_k \in \{0, 1\}$  was used to track the completion of the exercised subtask,  
524 with 1 meaning that the subtask was performed successfully and 0 meaning failure. The  
525 observation model for  $n_k$  was assumed to be a Bernoulli probability model:

$$Pr(n_k | p_k) = p_k^{n_k} (1 - p_k)^{1 - n_k} \quad (3)$$

526 where  $p_k$ , the probability of performing the subtask successfully at repetition  $k$ , was related to  
527  $MI_k$  by a logistic function:

$$p_k = \frac{\exp(MI_k)}{1 + \exp(MI_k)} \quad (4)$$

528 ensuring that  $p_k$  was constrained in  $[0, 1]$ . Furthermore, this formulation guaranteed that  $p_k$   
529 would approach 1 with increasing MI.

530 The model parameters  $\{\alpha_j, \beta_j, \sigma_{\delta,j}, \sigma_{\square}, p_k\}$  were estimated for each individual subject using the  
531 recordings of  $r_{j,k}$  and  $n_k$  (i.e., kinematic recordings from the robotic device, see Section 2.4)  
532 and by applying Bayesian Monte Carlo Markov Chain methods. The estimation of the  
533 parameters resulted in an estimate for MI. In order to ensure accuracy of the model, it was  
534 necessary that the number of recordings of  $r_{j,k}$  and  $n_k$  exceeded the number of parameters.  
535 Based on simulations performed with varying number of data points (see *Supplementary*  
536 *material*), the minimum number of data points for MI estimation was set to 8. In order to

537 validate the capability of the proposed approach to appropriately capture variable dynamics of  
538 the performance measures, we simulated different rehabilitation scenarios under varying  
539 conditions (see *Supplementary material*). As we aimed at estimating MI at subtask level,  
540 separate MI models were used for each movement direction of the training exercise.

## 541 **5.2 Performance measures**

542 Previous studies have shown that mechanisms of post-stroke recovery can be described by  
543 factors related to movement speed, smoothness, and efficiency [28, 47, 49]. Unlike  
544 physiological signals, these kinematic performance measures can be easily recorded and  
545 processed in real-time, promoting their use in clinical settings. In this study, we selected two  
546 continuous performance variables  $r_j$  for the use with the MI model: i) the mean velocity of a  
547 movement (MV) and ii) the spectral arc length (SAL), a robust and consistent measure of  
548 movement smoothness [46]. SAL is a dimensionless measure quantifying movement  
549 smoothness by negative values, where higher absolute values are related to jerkier  
550 movements. Regarding rehabilitation training, values of SAL close to zero are desirable, as  
551 well as high values of MV. Both measures were computed from the Cartesian coordinates of  
552 the three-dimensional trajectory of the robotic handle (see section *D. Robotic exoskeleton and*  
553 *motor task*). The discrete variable  $n_k$ , instead, was denoted as success (SUCC) and defined  
554 separately for the experiments with the healthy participants and the patients. For the patients,  
555 the value of SUCC was determined by the robotic assistance (i.e., SUCC = 1 if the patient  
556 performed the movement without robotic assistance, SUCC = 0 otherwise). On the other  
557 hand, the healthy participants were expected not to rely on the robotic assistance, although it  
558 was also provided if necessary. This assumption was supported by preliminary experiments  
559 with healthy subjects (see *Supplementary*). Therefore, in order to have an equivalent discrete  
560 variable for the experiment with healthy subjects, we defined the value of SUCC based on the  
561 execution time (i.e., SUCC = 1 if a healthy participant completed the movement within the

562 time threshold  $t_{th}$ ,  $SUCC = 0$  otherwise). The time threshold  $t_{th}$  was set to 4 seconds based on  
563 preliminary experiments with healthy subjects (see *Supplementary*).

### 564 **5.3 Personalization routine**

565 Using the model described in the previous section, MI was continuously tracked for each  
566 subtask (i.e., single movement towards target, see Section 5.4) and used to implement a  
567 personalized training routine. At the beginning of the training, we identified the subject-  
568 specific difficulty level for each subtask of the training exercise based on an initial assessment  
569 of the performance measures. The subtasks were then ordered by increasing difficulty and the  
570 easiest ones were selected as the initial training set (see section 5.6 for details on the ordering  
571 of the single movements). During the training, a subtask was removed from the set of current  
572 training subtasks when the MI estimates for this movement exceeded a given threshold and  
573 approached a plateau. Specifically, the probability of performing the subtask successfully ( $p_k$ ,  
574 see Section 5.1) had to be greater than 0.5, and the difference between two consecutive MI  
575 values (i.e., between two repetitions of the same subtask) had to be smaller than 5% for at  
576 least four repetitions. Given the observation equation for  $p_k$ , the former condition ( $p_k > 0.5$ )  
577 can be equally expressed in terms of the motor improvement:  $MI_k > 0$ . Once these conditions  
578 were satisfied, the subtask was replaced by a more difficult one from the training queue. The  
579 removed subtask was placed back into the training queue, so that it could be reintroduced at a  
580 later stage.

### 581 **5.4 Robotic exoskeleton and motor task**

582 We implemented the motor improvement model and the personalization routine in the robotic  
583 upper-limb exoskeleton ALEx [39, 40]. During the experiments, the patient and the healthy  
584 participants were instructed to perform point-to-point reaching movements at their  
585 comfortable speed (Fig. 1a). All reaching movements started from the center of the workspace



586 and the goal was to reach one of the eighteen targets distributed over a sphere of 19 cm of  
587 radius (Fig. 1b). Each movement towards a target represented a subtask. This design allowed  
588 exploiting an extensive three-dimensional workspace and provided means to easily identify all  
589 subtasks of the exercise. The sphere was positioned so that its center was aligned with the  
590 acromion of the right arm mid-way between the center of the target panel and the subject's  
591 acromion. The targets were displayed on a screen mounted in front of the subjects and visual  
592 feedback was provided by means of a cursor mapping the position of the exoskeleton's handle  
593 to the screen. In order to preserve the depth perception, the dimensions of the target spheres  
594 were modified in accordance with their position in the 3D space. If a subject was unable to  
595 reach a target (i.e., the subject did not move for more than 3 seconds), ALEx activated its  
596 assistance mode to guide the subject towards the target according to a minimum jerk speed  
597 profile [62].

## 598 **5.5 Participants**

### 599 **5.5.1 Healthy participants**

600 Seventeen right-handed subjects (eight males, nine females,  $25.4 \pm 3.3$  years old) participated  
601 in the experimental validation of our approach. The participants did not present any evidence  
602 or known history of skeletal and neurological diseases and they exhibited normal ranges of  
603 motion and muscle strength. All participants gave their informed consent to participate in the  
604 study, which had been previously approved by the Commission Cantonale d'Éthique de la  
605 Recherche Genève (CCER, Geneva, Switzerland, 2017-00504).

### 606 **5.5.2 Subacute stroke patients**

607 Two subacute stroke patients from the inpatient unit of the Hôpitaux Universitaires de Genève  
608 (HUG, Geneva, Switzerland) were included in the study. A summary of the patient  
609 information is reported in Table 1. Both patients suffered from a right hemiplegia with at least  
610  $10^\circ$  of residual motion in shoulder and elbow joints. The patients were enrolled in the study

611 within two to eight weeks after the stroke and underwent a therapy following the adaptive  
612 robotic rehabilitation protocol described in section 5.6. The patients received the robot-aided  
613 treatment in addition to a standard non-robotic rehabilitation therapy: each patient received  
614 two sessions of 30 minutes of physical therapy per day, five days per week, as well as five  
615 sessions of 30 minutes of occupational therapy per week, on an inpatient basis, for 8 to 16  
616 weeks. This was followed by an outpatient treatment of 1-4 hours of physical and  
617 occupational therapy per week. All patients gave their informed consent to participate in the  
618 study. This study is registered in ClinicalTrials.gov (NCT02770300) and the experimental  
619 protocols were approved by Swissmedic and Swissethics.

620 Table 1. Demographics and information of the stroke patients included in the study

621

Patient	Gender	Age	Weight (kg)	Height (cm)	Hand Dominancy	Enrolment after lesion
<i>P01</i>	Male	86	66	165	right	3 weeks
<i>P02</i>	Male	65	81	180	right	2 weeks

## 622 **5.6 Experimental protocols**

### 623 **5.6.1 Healthy participants**

624 The healthy participants attended a single experimental session, which comprised seven  
625 blocks of reaching movements (Fig. 1c). Breaks were allowed between the blocks to prevent  
626 fatigue. The session started with an initial assessment block consisting of three runs ( $A_{I,1-3}$ ).  
627 During each run all 18 targets were presented once and in a randomized order. The purpose of  
628 the assessment block was i) to allow familiarization with the robotic system and the motor  
629 task and ii) to record a baseline for the performance measures. This block was followed by  
630 five blocks  $B_{1-5}$  during which the visual feedback was inverted (i.e., an upward movement was  
631 displayed as downward and vice versa, likewise for left/right and forward/backward  
632 movements). This visual manipulation was introduced to induce motor performances with  
633 temporal dynamics resembling the ones observed in robot-aided rehabilitation of stroke  
634 patients [28, 37, 38]. At the onset of the five inversion blocks, participants were not informed

635 about the manipulation of the visual feedback, but they were told that the task difficulty was  
636 changed. Each of the five inversion blocks  $B_{1-5}$  consisted of five runs, each one composed of  
637 eight point-to-point reaching movements for a total of 40 reaching movements per block.

638 The initial set of training targets for each participant was generated following a semi-  
639 randomized procedure: it always contained the six on-axis targets (i.e., targets 1, 3, 5, 7, 10  
640 and 13, see Fig. 1b) and two randomly selected off-axis targets (i.e., targets 2, 4, 6, 8, 11, 14,  
641 15, 16, 17 and 18). The presentation order of the eight initial training targets was randomized.  
642 The remaining ten off-axis targets were placed randomly in the training queue. Previous  
643 studies using planar setups [33, 63] demonstrated that participants showed better performance  
644 for targets lying on the axis perpendicular to the inversion. Although in this study we used a  
645 three-dimensional setup, we also hypothesized that participants would have less difficulty  
646 with the on-axis targets, as they involved inversions in only one dimension (in contrast to  
647 inversions in two dimensions for the off-axis targets).

648 During the five inversion blocks  $B_{1-5}$ , a target was removed from the current set of training  
649 targets if the MI estimates for this subtask satisfied the replacement conditions (see section  
650 5.3). In this case, the target was replaced by the next one in the training queue. The inversion  
651 blocks  $B_{1-5}$  were followed by a final assessment block which was composed of three runs  
652 ( $A_{F,1-3}$ ) and followed the same procedure as the initial assessment block (i.e., neither visual  
653 manipulation nor personalization were applied). The data acquired during the assessment  
654 blocks (i.e.,  $A_{I,1-3}$  and  $A_{F,1-3}$ ) were not considered for the MI estimation.

### 655 **5.6.2 Subacute stroke patients**

656 The experimental protocol for the patients consisted of four weeks of robot-aided  
657 rehabilitation therapy (Fig. 1d), with three sessions of 30 minutes per week. The training  
658 comprised the regular point-to-point reaching task (see section 5.4). In order to evaluate the  
659 outcome of their rehabilitation training, the patients completed two assessment sessions

660 before ( $A_{I,1-2}$ ) and after ( $A_{F,1-2}$ ) the therapy. The initial assessment sessions  $A_{I,1-2}$  were  
661 completed two weeks and one week before the beginning of the therapy. The final assessment  
662 sessions  $A_{F,1-2}$  were completed one week and one month after the end of the therapy. During  
663 the initial and final assessment sessions, all eighteen targets of the point-to-point reaching task  
664 were presented to the patients in a randomized order. The total amount of reaching  
665 movements for each session was determined by the physical therapist while encouraging the  
666 patient to perform as many movements as possible. In addition, the patients were evaluated  
667 using the upper extremity section of the Fugl-Meyer assessment (FMA-UE, [64]).

668 For the treatment sessions, we first identified the patient-specific difficulty for each of the 18  
669 targets following the initial assessment sessions  $A_{I,1-2}$ . Specifically, we analyzed the mean  
670 values of MV, SAL and SUCC for each of the eighteen training targets. The targets were first  
671 ordered by descending (i.e., starting from easier targets) mean values of SUCC (rate of  
672 SUCC). If several targets had equal values for the rate of SUCC, the order amongst them was  
673 determined by their mean values for MV and SAL, while giving both measures equal weight.  
674 The first eight targets of the resulting list were selected as the initial training targets. The  
675 remaining targets were placed in a training queue while conserving the determined order of  
676 difficulty. During the therapy ( $W_1$ - $W_4$ , see Fig. 1), MI was continuously estimated for each  
677 training target separately. The replacement of a training target based on the MI estimates  
678 followed the procedure presented in Section 5.3. The current set of training targets was saved  
679 after the completion of each training session, ensuring continuity between sessions. The total  
680 amount of reaching movements for each session was determined by the physical therapist  
681 while encouraging the patient to perform as many movements as possible.

## 682 **5.7 Statistical analysis**

683 A two-sample t-test was used to compare the performance differences between two groups  
684 within the healthy population (fast and slow adapters). A two-way ANOVA was used to

685 assess the interaction effects of visual manipulation (introduced between  $A_3$  and  $B_1$ ) and  
686 adaptation speed (fast and slow adapters) in healthy participants. A paired t-test was used to  
687 compare the performances between different time points for the patients performing the pilot  
688 test. A significance level of 0.05 was used for all analyses. All analyses were performed using  
689 MATLAB (The MathWorks, Natick, Massachusetts).

## 690 **List of abbreviations**

691	MI	Motor improvement
692	MV	Movement velocity
693	SAL	Spectral arc length
694	SUCC	Success
695	FMA-UE	Fugl-Meyer assessment for upper extremities

## 696 **Declarations**

### 697 **Ethics approval and consent to participate**

698 All participants gave their informed consent to participate in the study, which had been  
699 previously approved by the Commission Cantonale d'Éthique de la Recherche Genève  
700 (CCER, Geneva, Switzerland, 2017-00504).

### 701 **Consent for publication**

702 All participants signed an informed consent to the use of all coded data collected during the  
703 study in scientific publications.

### 704 **Availability of data and material**

705 Since the data used in this study includes data collected in a clinical trial with patients, the

706 data will not be shared.

### 707 **Competing interests**

708 The authors declare that there is no conflict of interest.

### 709 **Funding**

710 This study was partly funded by the Wyss Center for Bio and Neuroengineering, the Swiss

711 National Competence Center in Robotics and the Bertarelli Foundation.

### 712 **Authors' contributions**

713 C.G. designed the model, carried out experiments, analysed data and wrote the paper;

714 E.P. designed the model, carried out experiments, analysed data and wrote the paper;

715 N.K. designed the model, carried out experiments, analysed data and wrote the paper;

716 C.P. designed the model, carried out experiments, analysed data and wrote the paper;

717 A.P. designed the model and wrote the paper;

718 M.C. carried out experiments and wrote the paper;

719 J.M. carried out experiments and wrote the paper;

720 C.M. carried out experiments and wrote the paper;

721 P.N. carried out experiments and wrote the paper;

722 A.G. designed the model and wrote the paper;

723 S.M. designed the model and wrote the paper;

### 724 **Acknowledgements**

725 The authors would like to thank all the volunteers and the patients enrolled in the study. We

726 would also like to thank Wearable Robotics and PERCRO for their support and expertise.

## 727 **References**

- 728 1. Donnan GA, Fisher M, Macleod M, Davis SM (2008) Stroke. *Lancet* 371:1612–23
- 729 2. Langhorne P, Coupar F, Pollock A (2009) Motor recovery after stroke: a systematic  
730 review. *Lancet Neurol* 8:741–754
- 731 3. Lawrence ES, Coshall C, Dundas R, Stewart J, Rudd AG, Howard R, Wolfe CDA  
732 (2001) Estimates of the Prevalence of Acute Stroke Impairments and Disability in a  
733 Multiethnic Population. *Stroke* 32:1279–1284
- 734 4. Carod-Artal J, Egido JA, Gonzalez JL, Varela de Seijas E (2000) Quality of Life  
735 Among Stroke Survivors Evaluated 1 Year After Stroke □: Experience of a Stroke Unit.  
736 *Stroke* 31:2995–3000
- 737 5. Clarke P, Marshall V, Black SE, Colantonio A (2002) Findings From the Canadian  
738 Study of Health and Aging. *Stroke* 33:1016–1021
- 739 6. Veerbeek JM, Langbroek-Amersfoort AC, van Wegen EEH, Meskers CGM, Kwakkel  
740 G (2017) Effects of Robot-Assisted Therapy for the Upper Limb After Stroke.  
741 *Neurorehabil Neural Repair* 31:107–121
- 742 7. Dobkin BH (2004) Strategies for stroke rehabilitation. *Lancet Neurol* 3:528–536
- 743 8. Marchal-Crespo L, Reinkensmeyer DJ (2009) Review of control strategies for robotic  
744 movement training after neurologic injury. *J Neuroeng Rehabil* 6:20
- 745 9. Di Pino G, Pellegrino G, Assenza G, et al (2014) Modulation of brain plasticity in  
746 stroke: a novel model for neurorehabilitation. *Nat Rev Neurol* 10:597–608
- 747 10. Wagner TH, Lo AC, Peduzzi P, et al (2011) An economic analysis of robot-assisted  
748 therapy for long-term upper-limb impairment after stroke. *Stroke* 42:2630–2632
- 749 11. Klamroth-Marganska V, Blanco J, Campen K, et al (2014) Three-dimensional, task-  
750 specific robot therapy of the arm after stroke: A multicentre, parallel-group randomised  
751 trial. *Lancet Neurol* 13:159–166
- 752 12. Lo AC, Guarino PD, Richards LG, et al (2010) Robot-Assisted Therapy for Long-Term  
753 Upper-Limb Impairment after Stroke. *N Engl J Med* 362:1772–1783
- 754 13. Grimm F, Naros G, Gharabaghi A (2016) Closed-loop task difficulty adaptation during  
755 virtual reality reach-to-grasp training assisted with an exoskeleton for stroke  
756 rehabilitation. *Front Neurosci* 10:1–13
- 757 14. Krakauer JW (2006) Motor learning: its relevance to stroke recovery and  
758 neurorehabilitation. *Curr Opin Neurol* 19:84–90
- 759 15. Guadagnoli MA, Lee TD (2004) Challenge Point: A Framework for Conceptualizing  
760 the Effects of Various Practice Conditions in Motor Learning. *J Mot Behav* 36:212–  
761 224
- 762 16. Rosenthal O, Wing AM, Wyatt JL, Punt D, Brownless B, Ko-Ko C, Miall RC (2019)  
763 Boosting robot-assisted rehabilitation of stroke hemiparesis by individualized selection

- 764 of upper limb movements - A pilot study. *J Neuroeng Rehabil* 16:1–14
- 765 17. Krebs HI, Palazzolo JJ, Dipietro L, Ferraro M, Krol J, Ranekleiv K, Volpe BT, Hogan  
766 N (2003) Rehabilitation robotics: Performance-based progressive robot-assisted  
767 therapy. *Auton Robots* 15:7–20
- 768 18. Kan P, Huq R, Hoey J, Goetschalckx R, Mihailidis A (2011) The development of an  
769 adaptive upper-limb stroke rehabilitation robotic system. *J Neuroeng Rehabil* 8:33
- 770 19. Papaleo E, Zollo L, Spedaliere L, Guglielmelli E (2013) Patient-tailored adaptive  
771 robotic system for upper-limb rehabilitation. *Proc - IEEE Int Conf Robot Autom* 3860–  
772 3865
- 773 20. Metzger J-C, Lamercy O, Califfi A, Dinacci D, Petrillo C, Rossi P, Conti FM, Gassert  
774 R (2014) Assessment-driven selection and adaptation of exercise difficulty in robot-  
775 assisted therapy: a pilot study with a hand rehabilitation robot. *J Neuroeng Rehabil*  
776 11:154
- 777 21. Wittmann F, Lamercy O, Gonzenbach RR, Van Raai MA, Hover R, Held J, Starkey  
778 ML, Curt A, Luft A, Gassert R (2015) Assessment-driven arm therapy at home using  
779 an IMU-based virtual reality system. *IEEE Int Conf Rehabil Robot* 2015-Sept:707–  
780 712
- 781 22. Wu W, Wang D, Wang T, Liu M (2017) A personalized limb rehabilitation training  
782 system for stroke patients. *2016 IEEE Int Conf Robot Biomimetics, ROBIO 2016*  
783 1924–1929
- 784 23. Wolbrecht ET, Chan V, Reinkensmeyer DJ, Bobrow JE (2008) Optimizing compliant,  
785 model-based robotic assistance to promote neurorehabilitation. *IEEE Trans Neural Syst*  
786 *Rehabil Eng* 16:286–297
- 787 24. Octavia JR, Coninx K (2014) Adaptive personalized training games for individual and  
788 collaborative rehabilitation of people with multiple sclerosis. *Biomed Res Int*. doi:  
789 10.1155/2014/345728
- 790 25. Rodriguez Guerrero C, Fraile Marinero J, Perez Turiel J, Rivera Farina P (2010) Bio  
791 cooperative robotic platform for motor function recovery of the upper limb after stroke.  
792 *2010 Annu Int Conf IEEE Eng Med Biol Soc EMBC'10* 4472–4475
- 793 26. Novak D, Mihelj M, Zihel J, Olensek A, Munih M (2011) Psychophysiological  
794 measurements in a biocooperative feedback loop for upper extremity rehabilitation.  
795 *IEEE Trans Neural Syst Rehabil Eng* 19:400–410
- 796 27. Badesa FJ, Morales R, Garcia-Aracil NM, Sabater JM, Zollo L, Papaleo E,  
797 Guglielmelli E (2016) Dynamic Adaptive System for Robot-Assisted Motion  
798 Rehabilitation. *IEEE Syst J* 10:984–991
- 799 28. Panarese A, Colombo R, Sterpi I, Pisano F, Micera S (2012) Tracking Motor  
800 Improvement at the Subtask Level During Robot-Aided Neurorehabilitation of Stroke  
801 Patients. *Neurorehabil Neural Repair* 26:822–833
- 802 29. Smith AC (2004) Dynamic Analysis of Learning in Behavioral Experiments. *J*  
803 *Neurosci* 24:447–461



- 804 30. Prerau MJ, Smith AC, Eden UT, Kubota Y, Yanike M, Suzuki W, Graybiel AM,  
805 Brown EN (2009) Characterizing Learning by Simultaneous Analysis of Continuous  
806 and Binary Measures of Performance. *J Neurophysiol* 102:3060–3072
- 807 31. Rinne P, Hassan M, Fernandes C, et al (2017) Motor dexterity and strength depend  
808 upon integrity of the attention-control system. *Proc Natl Acad Sci* 201715617
- 809 32. Shabbott BA, Sainburg RL (2010) Learning a visuomotor rotation: Simultaneous visual  
810 and proprioceptive information is crucial for visuomotor remapping. *Exp Brain Res*  
811 203:75–87
- 812 33. Werner S, Bock O (2010) Mechanisms for visuomotor adaptation to left-right reversed  
813 vision. *Hum Mov Sci* 29:172–178
- 814 34. Krakauer JW (2009) Motor learning and consolidation: the case of visuomotor rotation.  
815 *Adv Exp Med Biol* 629:405–421
- 816 35. Miall RC, Jenkinson N, Kulkarni K (2004) Adaptation to rotated visual feedback: A re-  
817 examination of motor interference. *Exp Brain Res* 154:201–210
- 818 36. Harris CS (1965) Perceptual adaptation to inverted, reversed, and displaced vision.  
819 *Psychol Rev* 72:419–444
- 820 37. Colombo R, Pisano F, Micera S, Mazzone A, Delconte C, Carrozza MC, Dario P,  
821 Minuco G (2008) Assessing mechanisms of recovery during robot-aided  
822 neurorehabilitation of the upper limb. *Neurorehabil Neural Repair* 22:50–63
- 823 38. Colombo R, Sterpi I, Mazzone A, Delconte C, Minuco G, Pisano F (2010) Measuring  
824 changes of movement dynamics during robot-aided neurorehabilitation of stroke  
825 patients. *IEEE Trans Neural Syst Rehabil Eng* 18:75–85
- 826 39. Bergamasco M, Salsedo F, Lenzo B (2013) An exoskeleton structure for physical  
827 interaction with a human being.
- 828 40. Pirondini E, Coscia M, Marcheschi S, Roas G, Salsedo F, Frisoli A, Bergamasco M,  
829 Micera S (2016) Evaluation of the effects of the Arm Light Exoskeleton on movement  
830 execution and muscle activities: a pilot study on healthy subjects. *J Neuroeng Rehabil*  
831 13:9
- 832 41. Coscia M, Cheung V, Tropea P, Koenig A, Monaco V, Bennis C, Micera S, Bonato P  
833 (2014) The effect of arm weight support on upper limb muscle synergies during  
834 reaching movements. *J Neuroeng Rehabil* 11:1–15
- 835 42. Frisoli A, Borelli L, Montagner A, Marcheschi S, Procopio C, Salsedo F, Bergamasco  
836 M, Carboncini MC, Tolaini M, Rossi B (2007) Arm rehabilitation with a robotic  
837 exoskeleton in Virtual Reality. 2007 IEEE 10th Int Conf Rehabil Robot ICORR'07  
838 00:631–642
- 839 43. Krebs HI, Ferraro M, Buerger SP, Newbery MJ, Makiyama A, Sandmann M, Lynch D,  
840 Volpe BT, Hogan N (2004) Rehabilitation robotics: pilot trial of a spatial extension for  
841 MIT-Manus. *J Neuroeng Rehabil* 1:5
- 842 44. Biernaskie J (2004) Efficacy of Rehabilitative Experience Declines with Time after

- 843 Focal Ischemic Brain Injury. *J Neurosci* 24:1245–1254
- 844 45. Cramer SC (2008) Repairing the human brain after stroke: I. Mechanisms of  
845 spontaneous recovery. *Ann Neurol* 63:272–287
- 846 46. Balasubramanian S, Melendez-Calderon A, Burdet E (2012) A robust and sensitive  
847 metric for quantifying movement smoothness. *IEEE Trans Biomed Eng* 59:2126–2136
- 848 47. Bosecker C, Dipietro L, Volpe B, Igo Krebs H (2010) Kinematic Robot-Based  
849 Evaluation Scales and Clinical Counterparts to Measure Upper Limb Motor  
850 Performance in Patients With Chronic Stroke. *Neurorehabil Neural Repair* 24:62–69
- 851 48. Nordin N, Xie SQ, Wunsche B (2014) Assessment of movement quality in robot-  
852 assisted upper limb rehabilitation after stroke: a review. *J Neuroeng Rehabil* 11:137
- 853 49. Panarese A, Pirondini E, Tropea P, Cesqui B, Posteraro F, Micera S (2016) Model-  
854 based variables for the kinematic assessment of upper-extremity impairments in post-  
855 stroke patients. *J Neuroeng Rehabil* 13:81
- 856 50. Lang CE, Bland MD, Bailey RR, Schaefer SY, Birkenmeier RL (2013) Assessment of  
857 upper extremity impairment, function, and activity after stroke: Foundations for clinical  
858 decision making. *J Hand Ther* 26:104–115
- 859 51. Milot M, Spencer SJ, Chan V, Allington JP, Klein J, Chou C, Bobrow JE, Cramer SC,  
860 Reinkensmeyer DJ (2013) A crossover pilot study evaluating the functional outcomes  
861 of two different types of robotic movement training in chronic stroke survivors using  
862 the arm exoskeleton BONES. 1–12
- 863 52. Lillicrap TP, Moreno-Briseño P, Diaz R, Tweed DB, Troje NF, Fernandez-Ruiz J  
864 (2013) Adapting to inversion of the visual field: A new twist on an old problem. *Exp*  
865 *Brain Res* 228:327–339
- 866 53. Maclean N, Pound P, Wolfe C, Rudd A (2000) Qualitative analysis of stroke patients’  
867 motivation for rehabilitation. *Bmj* 321:1051–1054
- 868 54. Maclean N, Pound P, Wolfe C, Rudd A (2002) The Concept of Patient Motivation: A  
869 Qualitative Analysis of Stroke Professionals’ Attitudes Niall Maclean, Pandora Pound,  
870 Charles Wolfe and Anthony Rudd. 444–449
- 871 55. Colombo R, Pisano F, Mazzone A, Delconte C, Micera S, Carrozza MC, Dario P,  
872 Minuco G (2007) Design strategies to improve patient motivation during robot-aided  
873 rehabilitation. *J Neuroeng Rehabil* 4:3
- 874 56. Lee JY, Oh Y, Kim SS, Scheidt RA, Schweighofer N (2016) Optimal Schedules in  
875 Multitask Motor Learning. *Neural Comput* 28:667–685
- 876 57. Dipietro L, Krebs HI, Fasoli SE, Volpe BT, Stein J, Bever C, Hogan N (2007)  
877 Changing Motor Synergies in Chronic Stroke. *J Neurophysiol* 98:757–768
- 878 58. Dipietro L, Krebs HI, Fasoli SE, Volpe BT, Hogan N (2009) Submovement changes  
879 characterize generalization of motor recovery after stroke. *Cortex* 45:318–324
- 880 59. Kwakkel G, Kollen B, Twisk J (2006) Impact of time on improvement of outcome after

- 881 stroke. *Stroke* 37:2348–2353
- 882 60. Murphy TH, Corbett D (2009) Plasticity during stroke recovery: From synapse to  
883 behaviour. *Nat Rev Neurosci* 10:861–872
- 884 61. Zeiler SR, Krakauer JW (2013) The interaction between training and plasticity in the  
885 poststroke brain. *Curr Opin Neurol* 26:609–616
- 886 62. Sadaka-Stephan A, Pirondini E, Coscia M, Micera S (2015) Influence of trajectory and  
887 speed profile on muscle organization during robot-aided training. *IEEE Int Conf*  
888 *Rehabil Robot* 2015-Sept:241–246
- 889 63. Cunningham HA, Pavel M (1991) Target axis effects under transformed visual-motor  
890 mappings. *Pict Commun real virtual Environ* 283–304
- 891 64. Fugl-Meyer AR, Jääskö L, Leyman I, Olsson S, Steglind S (1975) The post-stroke  
892 hemiplegic patient. 1. a method for evaluation of physical performance. *Scand J*  
893 *Rehabil Med* 7:13–31

## 894 **Figure captions**

895 **Figure 1.** Experimental setup and protocols. (a) Schematic overview of experimental setup.  
896 (b) Design of the three-dimensional point-to-point reaching task. Eighteen targets  
897 (representing the different subtasks) are positioned over a sphere of 19 cm of radius (equally  
898 distributed on the three planes). The empty circle represents the center of the workspace  
899 (starting position). (c) Experimental protocol for healthy participants. Experiments were  
900 completed in a single session and were divided into blocks (one initial assessment block  $A_{I,1-3}$ ,  
901 five inversion blocks  $B_{1-5}$ , one final assessment block  $A_{F,1-3}$ ). The assessment blocks consisted  
902 of three runs, each composed of 18 reaching movements (one towards each target). The  
903 inversion blocks consisted of five runs, each composed of eight reaching movements. The  
904 training targets for the inversion blocks were automatically selected by the implemented  
905 personalization routine. Breaks were allowed between the blocks to prevent fatigue. (d)  
906 Experimental protocol for the patient. During the initial ( $A_{I,1-2}$ ) and final ( $A_{F,1-2}$ ) assessment  
907 sessions, all eighteen targets were presented to the patient. For each treatment session eight  
908 training targets were selected by the implemented personalization routine. The total number of  
909 repetitions performed in each session was determined by the physical therapist.

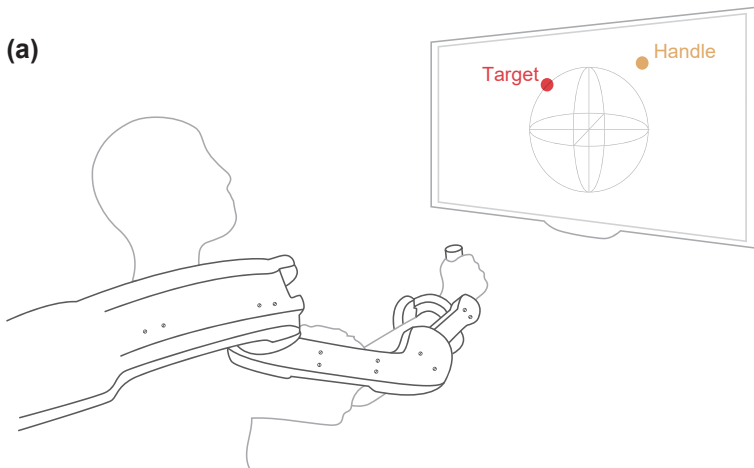
910 **Figure 2.** Analysis of performance measures for the experiment with healthy participants.  
911 Average values of mean velocity (MV, panel a), spectral arc length (SAL, panel b) and rate of  
912 SUCC (panel c) for each run (eight reaching movements) of fast (red) and slow (grey)  
913 adapters. Measures were averaged for all targets presented during a run and for all subjects of  
914 a group. Shaded areas depict standard error of the mean (sem). Vertical bars (panel d) depict  
915 the percentage of subjects in each group for which a target was replaced in B<sub>3-5</sub> or was not  
916 replaced at all. No targets were replaced in and B<sub>1-2</sub> due to lack of data needed for proper  
917 estimation of motor improvement.

918 **Figure 3.** Examples of MI estimates and performance measures at subtask level. Data is  
919 presented for a fast adapter and a slow adapter for the same two targets. Repetitions for each  
920 target are concatenated for all inversion blocks and presented in chronological order. Data for  
921 mean velocity (MV), spectral arc length (SAL) and MI were low-pass filtered for  
922 visualization purposes (raw data shown in light red/grey). Dotted lines depict one of the  
923 necessary conditions ( $MI > 0$ ) for triggering a target replacement. Green areas indicate the  
924 time span where the model detected a performance plateau and triggered a target replacement.  
925 Estimated model parameters ( $\alpha_j$ ,  $\beta_j$ ) for each target and subject are presented next to the  
926 corresponding MI curves (a summary and analysis on the model parameters can be found in  
927 the *Supplementary material*).

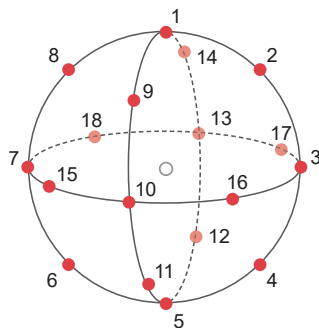
928 **Figure 4.** Summary of the results from the pilot test with two subacute stroke patients. (a)  
929 The first three rows show the mean values for mean velocity (MV), spectral arc length (SAL)  
930 and rate of success (SUCC) for each assessment and treatment session. Measures were  
931 averaged for all targets presented during a session, shaded areas depict standard error of the  
932 mean (SEM). The fourth row shows number of movements performed by the patients in each  
933 session. The fifth row shows the scores on the Fugl-Meyer scale for upper extremities (FMA-  
934 UE) for initial ( $A_{I,1-2}$ ) and final ( $A_{F,1-2}$ ) assessment sessions. The dotted line indicates the

935 maximum achievable score for FMA-UE (66 points). Last column shows changes for all  
936 metrics between the final assessments  $A_{F,1-2}$  and the second initial assessment  $A_{I,2}$ . Error bars  
937 depict standard error of the mean (SEM). Statistical significance between values are indicated  
938 by asterisks (\*,  $p < 0.05$ ) or dashes (-,  $p > 0.05$ ). (b) Summary of the training targets presented  
939 to the patients in each treatment session. Targets are listed by the order as presented to the  
940 patients (first eight targets from the top are the initial training set). (c) Analysis of  
941 performance measures for two different time points (i.e., before replacement and after  
942 reinsertion). The data shows the mean values for MV, SAL and SUCC averaged for all targets  
943 at these time points. Values are compared between the last four movements towards a training  
944 target before its replacement and the first four movements towards the target after it has been  
945 reinserted for training. Values are given relatively to the mean values obtained from the first  
946 four movements towards all targets. Error bars depict standard error of the mean (SEM).  
947 Statistical significance between values are indicated by asterisks (\*,  $p < 0.05$ ) or dashes (-,  $p >$   
948 0.05).

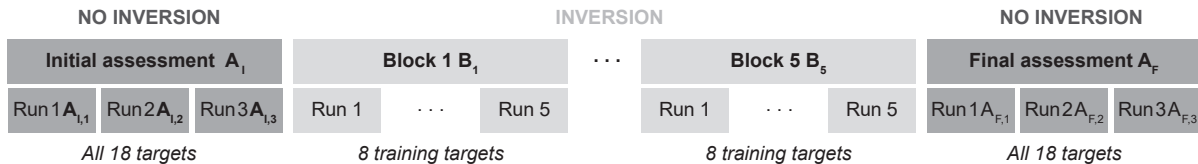
(a)



(b)

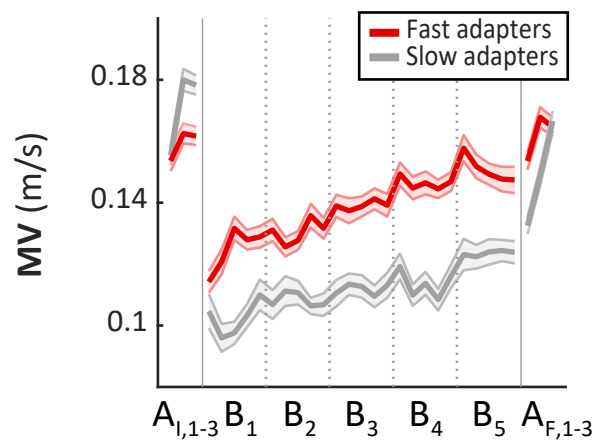
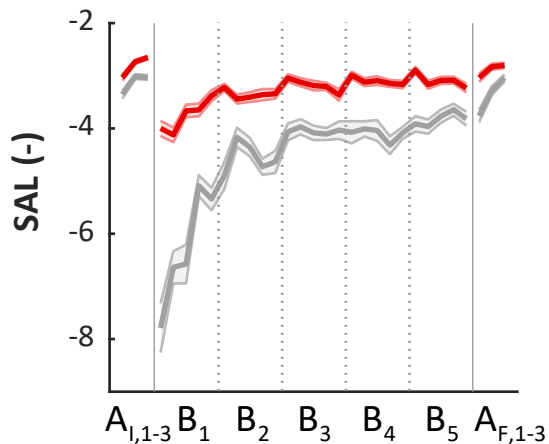
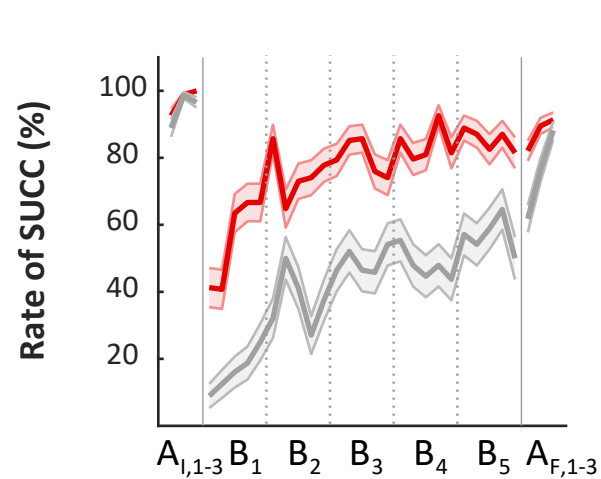
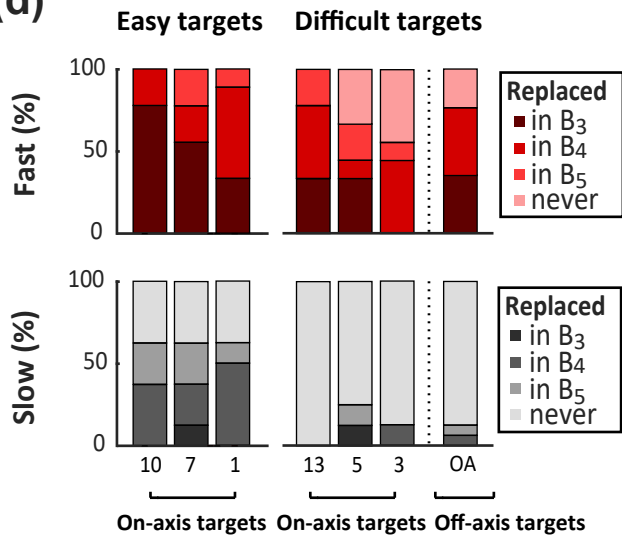


(c) Experimental protocol - Healthy participants

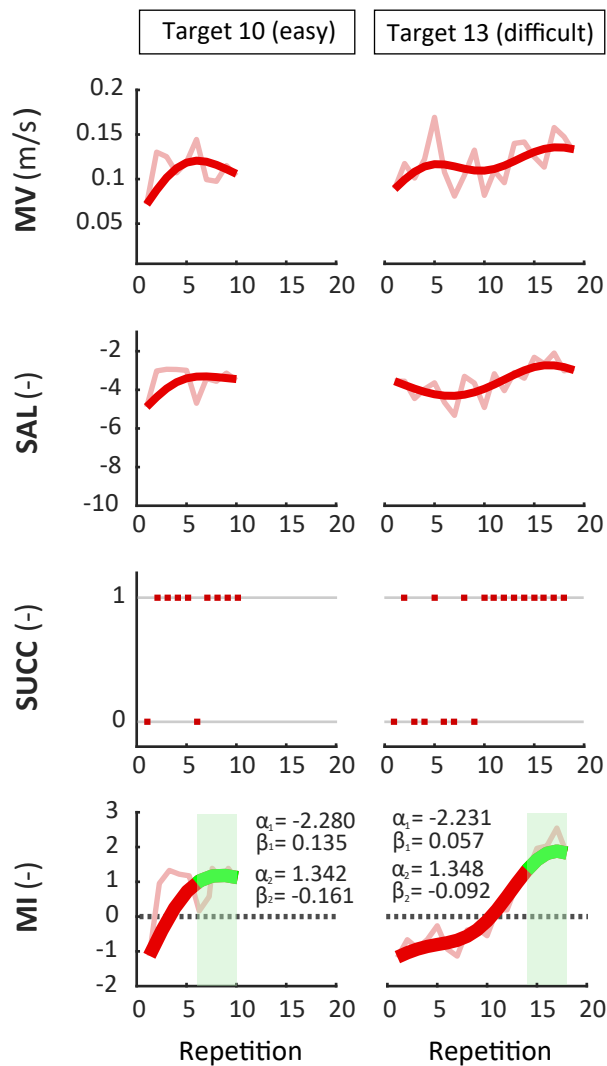


(d) Experimental protocol - Subacute stroke patients

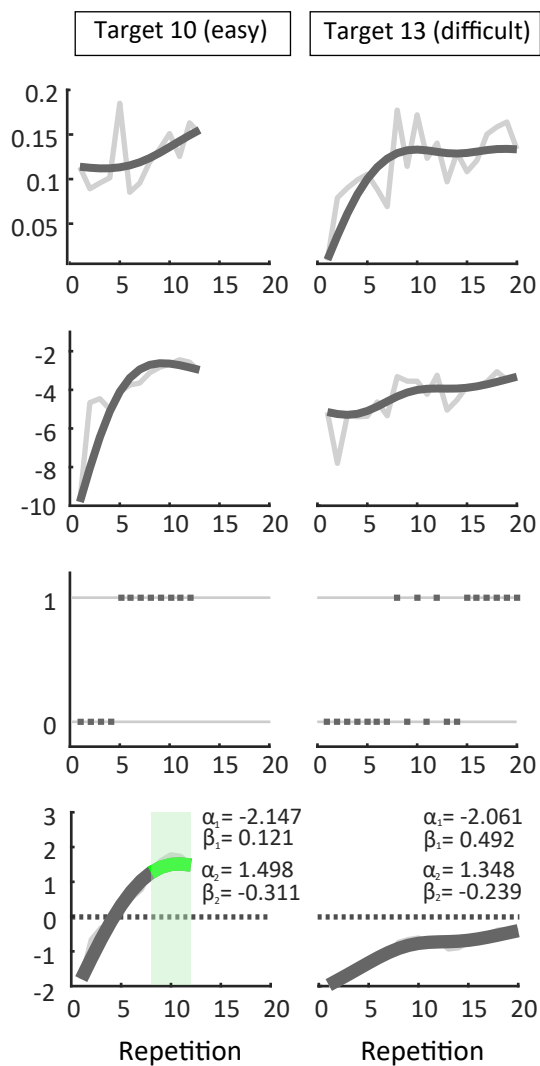


**(a)****(b)****(c)****(d)**

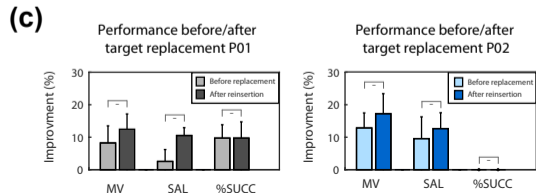
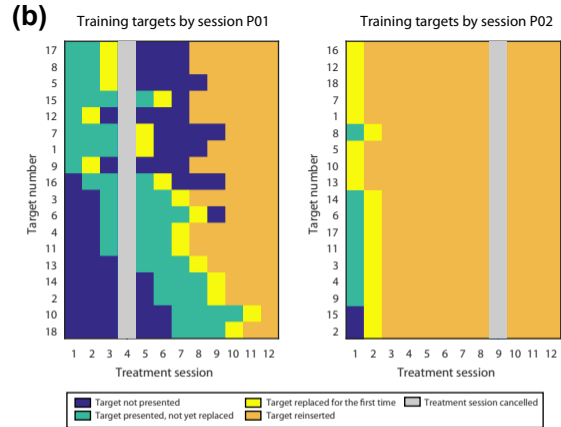
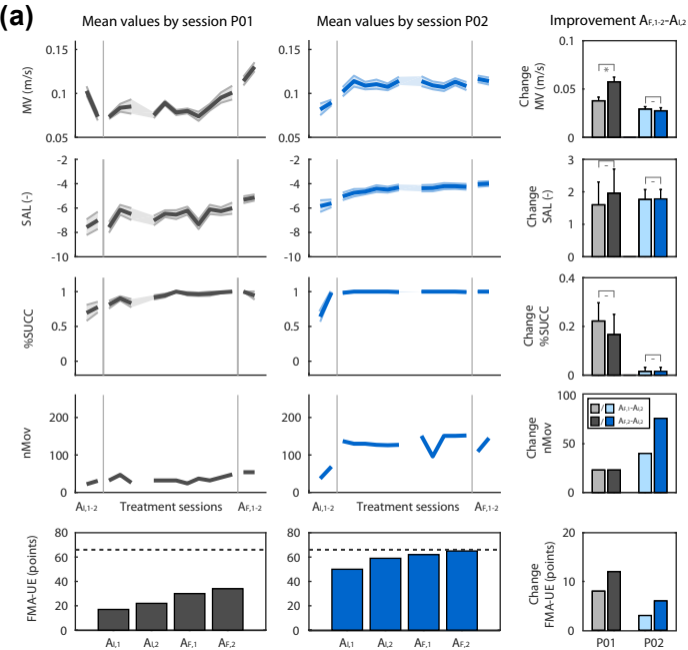
## Fast adapter

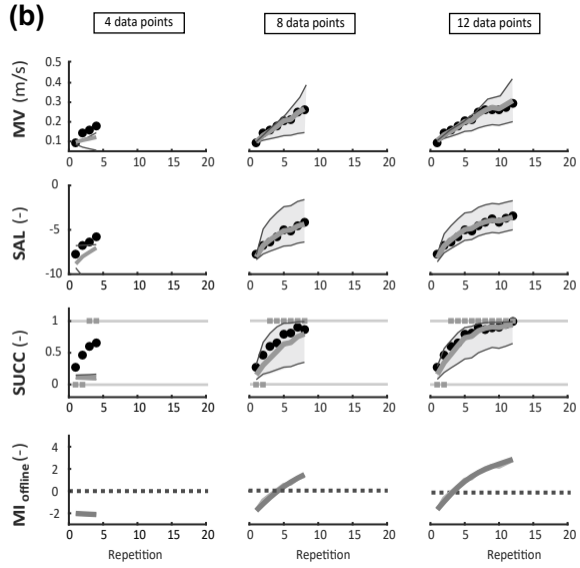
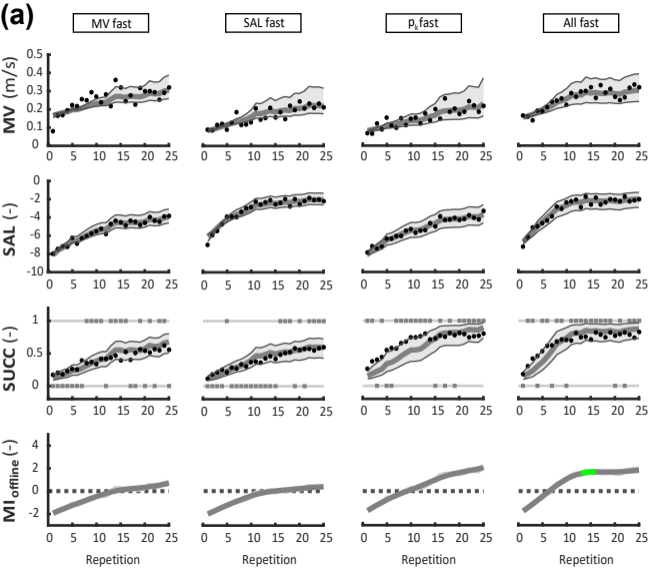


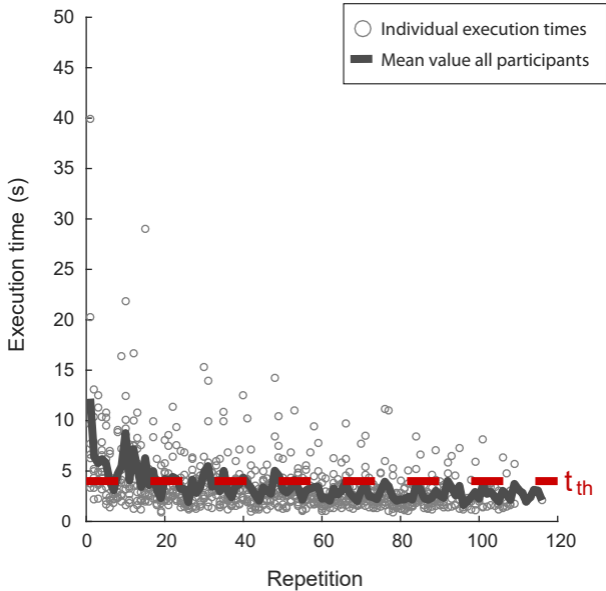
## Slow adapter





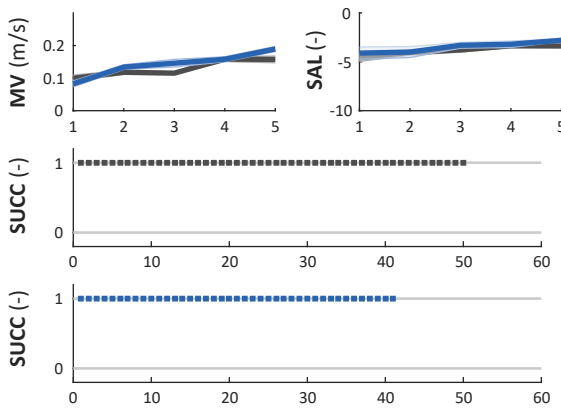




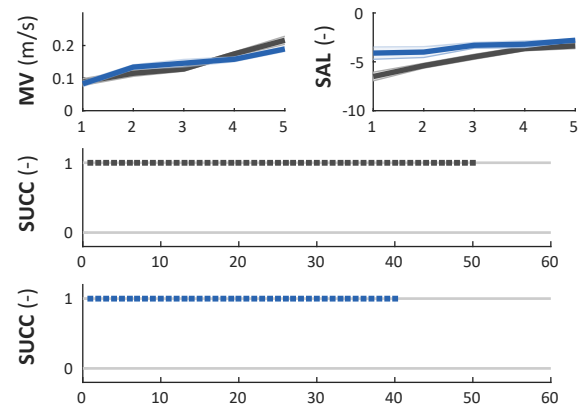


**PRE-001**

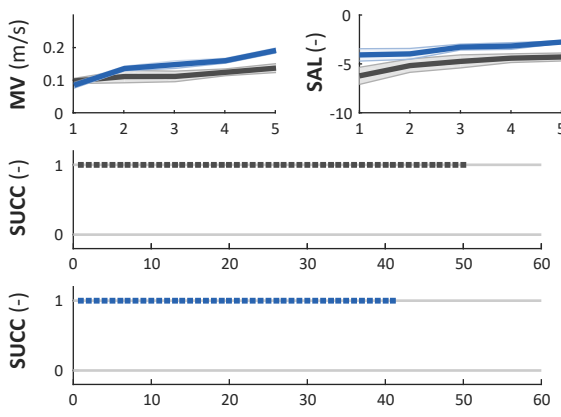
■ Depth  
■ No depth



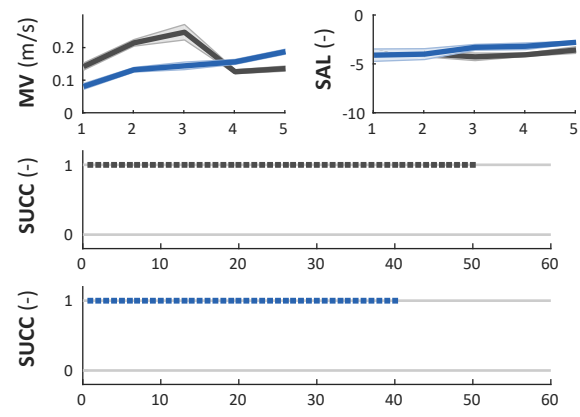
**PRE-002**



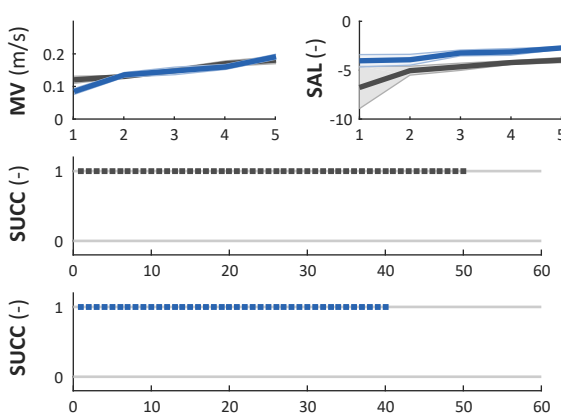
**PRE-003**



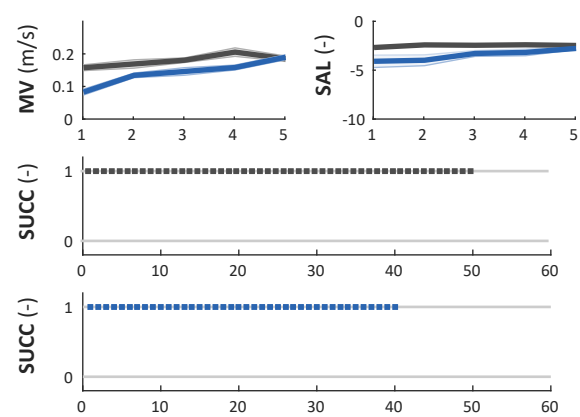
**PRE-004**



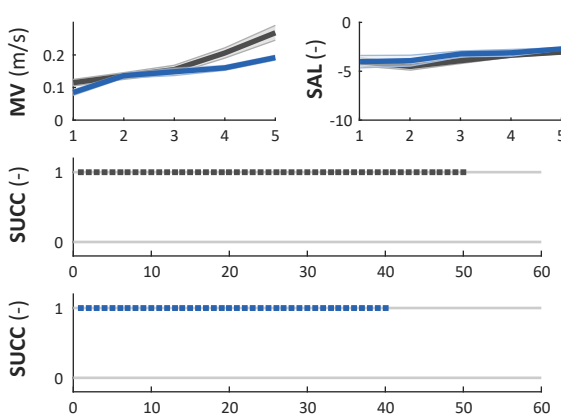
**PRE-005**



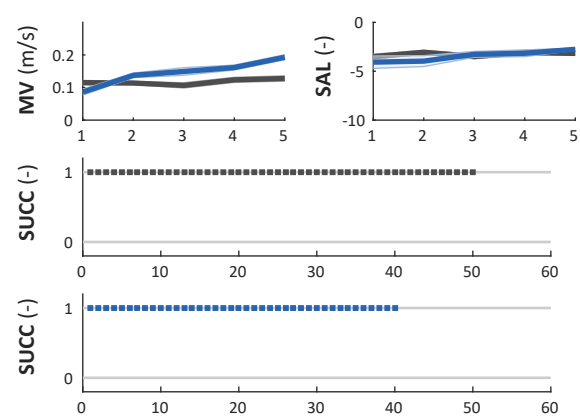
**PRE-006**

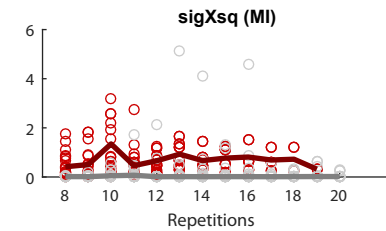
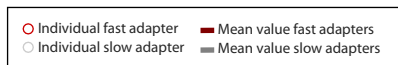
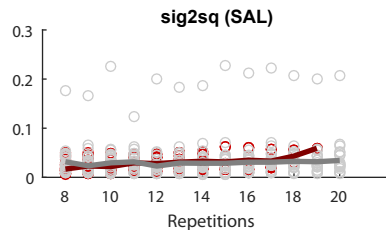
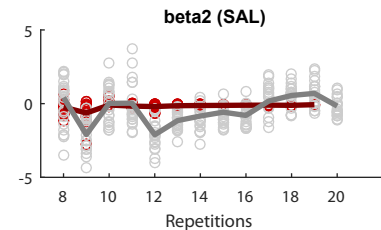
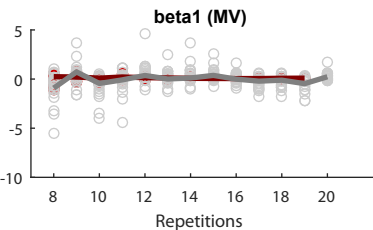
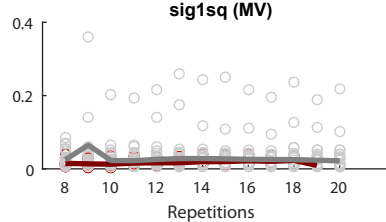
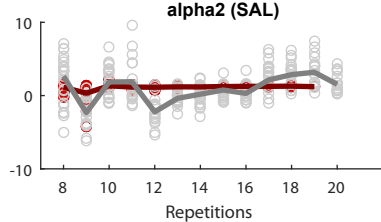
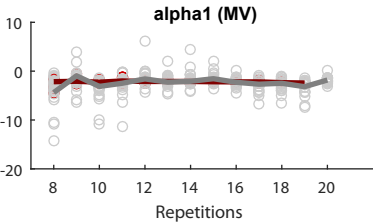


**PRE-007**

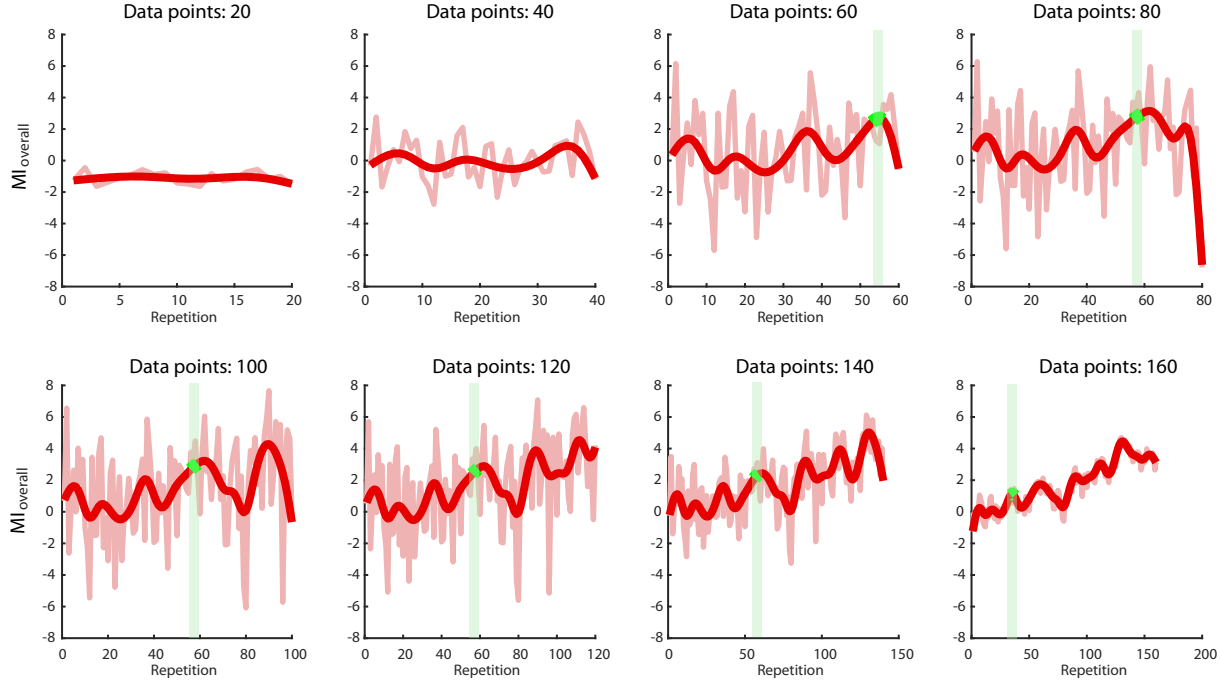


**PRE-008**





## Fast adapter



## Slow adapter

